Scaling of olfactory antennae of the terrestrial hermit crabs *Coenobita rugosus* and *Coenobita perlatus* during ontogeny

Lindsay D. Waldrop[1,2], **Roxanne M. Bantay**[2,3], **and Quang V. Nguyen**[2]

[1]**Dept. of Mathematics, Univ. of North Carolina at Chapel Hill**
[2]**Dept. of Integrative Biology, Univ. of California, Berkeley**
[3]**Dept. of Biology, San Francisco State Univ.**

ABSTRACT

Although many lineages of terrestrialized crustaceans have poor olfactory capabilities, crabs in the family Coenobitidae, including the terrestrial hermit crabs in the genus *Coenobita*, are able to locate food and water using olfactory antennae (antennules) to capture odors from the surrounding air. Terrestrial hermit crabs begin their lives as small marine larvae and must find a suitable place to undergo metamorphosis into a juvenile form, which initiates their transition to land. Juveniles increase in size by more than an order of magnitude to reach adult size. Since odor capture is a process heavily dependent on the size and speed of the antennules and physical properties of the fluid, both the transition from water to air and the large increase in size during ontogeny could impact odor capture. In this study, we examine two species of terrestrial hermit crabs, *Coenobita perlatus* H. Milne-Edwards and *Coenobita rugosus* H. Milne-Edwards, to determine how the antennule morphometrics and kinematics of flicking change in comparison to body size during ontogeny, and how this scaling relationship could impact odor capture by using a simple model of mass transport in flow. Many features of the antennules, including the chemosensory sensilla, scaled allometrically with carapace width and increased slower than expected by isometry, resulting in relatively larger antennules on juvenile animals. Flicking speed scaled as expected with isometry. Our mass-transport model showed that allometric scaling of antennule morphometrics and kinematics leads to thinner boundary layers of attached fluid around the antennule during flicking and higher odorant capture rates as compared to antennules which scaled isometrically. There were no significant differences in morphometric or kinematic measurements between the two species.

Keywords: hermit crab, sniffing, olfaction, Coenobita, terrestrialization, antennule

INTRODUCTION

Capturing chemical signals (odors) from the environment is an important task to many animals in both air and water. Crustaceans use the information derived from odors to find food and mates, identify conspecifics, and avoid predators (Dusenbery, 1992; Atema, 1995; Zimmer and Butman, 2000; Diaz et al., 1999; Pardieck et al., 1999; Ferner et al., 2005; Lecchini et al., 2010; Hazlett, 1969; Caldwell, 1979; Gleeson, 1980, 1982; Keller et al., 2003; Gherardi et al., 2005; Gherardi and Tricarico, 2007; Shabani et al., 2009; Skog, 2009; Welch et al., 1997). The olfactory organ of malacostracan crustaceans consists of chemosensory sensillae (aesthetascs) arranged in an array on the lateral flagellum each of their first antennae (antennules) (Fig. 1A). To capture odors, crustaceans move their antennules back and forth through the water in a motion called flicking (Fig. 1B-C). For aquatic crustaceans, each flick is a sniff, or the capture of a discrete sample of odor-containing water.

Many crustaceans, after moving onto land, have reduced or lost olfactory function in their antennules, few aesthetascs, and are unable to navigate by chemical signals (Bliss and Mantel, 1968; Greenaway, 2003). Although odor capture by terrestrial crustaceans is less understood as compared to aquatic crustaceans, there is evidence that crabs in the Family Coenobitidae are adept at locating a variety of odor sources in their environment including vegetable matter, detritus, and water (Thacker, 1996), as well as other non-traditional food items such as human feces and vomit (Barnes, 1997; Waldrop, 2012). Coenobitids have robust antennules with arrays of aesthetascs on the lateral flagella (Ghiradella et al.,

1968; Stensmyr et al., 2005) and wave their antennules in a flicking behavior similar to aquatic species (Stensmyr et al., 2005; Harzsch and Hansson, 2008). Coenobitids also have a large olfactory bulb, the site of olfactory information processing, similar in structure to the bulbs of insects (Beltz et al., 2003).

Despite their high level of terrestrialization, coenobitids are still tied to the ocean for reproduction, releasing marine larvae into the sea to develop (Greenaway, 2003). Competent larvae settle in the near-shore shallows and metamorphose into their juvenile, terrestrial form. This metamorphosis is followed by a transition to living exclusively on land (Brodie, 2002). The life history of coenobitids presents a unique challenge in terms of odor capture: these crabs must contend with both a change in size and a change in the fluid itself, both of which change the fluid dynamics of odor capture.

Fluid dynamics of odor capture

Crustaceans flick their antennules to generate convective flows around the sensory structures located on the antennules (Schmidt and Ache, 1979; Moore et al., 1991; Moore and Crimaldi, 2004; Goldman and Patek, 2002). When fluid moves across the antennule during flicking, a thin layer of fluid adheres to the surface of the antennule (the 'no-slip' condition); fluid between the layers attached to the antennule and surrounding environment is sheared and creates a velocity gradient from zero to the antennule's speed (u_∞) in a layer of fluid known as a boundary layer (Denny, 1993; Vogel, 1994).

The relative thickness of the boundary layer depends on the size and speed of the antennule as well as the physical properties of the fluid. In laminar flow, the relative boundary layer thickness (δ/L) is defined as the distance away from a moving object at which the speed of flow is less than 1% of the object's speed (u_∞), and for a flat plate moving through fluid:

$$\frac{\delta}{L} \propto \sqrt{\frac{\nu}{u_\infty L}} \propto Re^{-1/2} \tag{1}$$

where the Reynolds number (Re) is defined as

$$Re = \frac{u_\infty L}{\nu} \tag{2}$$

and relies on the distance from the leading edge of the plate (L) (Vogel, 1994; Denny, 1993). The fluid's kinematic viscosity (ν) in m^2s^{-1} describes how quickly momentum diffuses into the fluid of the boundary layer. The boundary layer prevents molecules from directly reaching the olfactory surface of the antennule, but increasing the antennule's speed will decrease the relative boundary layer thickness. A decrease in boundary layer thickness means a decrease in the distance between new odor-containing fluid and the antennule's surface (Moore et al., 1991; Koehl, 2006).

Since odor molecules cannot be delivered to the surface of the aesthetascs by fluid currents alone due to the entrained fluid layer, diffusion must transport molecules across the boundary layer (Stacey et al., 2002; Schuech et al., 2012). Diffusion is molecular movement by a random walk which causes a change in concentration over time. A change in concentration (C) with time (t) due to diffusion in one dimension (x) is described by Fick's law:

$$\frac{\partial C}{\partial t} = D\frac{\partial C}{\partial x} \tag{3}$$

where D is the substance's diffusivity coefficient in m^2s^{-1}. The higher the value of D, the more quickly molecules diffuse from their original point.

Scaling of odor-capture performance

As a terrestrial hermit crab grows, the increase in size and flicking speed and the change in fluid associated with the water-to-air transition will affect the ability of an animal to capture odor molecules. Odor capture will be affected in two major ways: the boundary layer over which diffusion must transport molecules and the relationship between diffusivities of a molecule in air and water.

The change in concentration away from an object (along x) can be thought of as proportional to the velocity gradient of the boundary layer around the antennule, as presented in Denny (1993):

$$\frac{\partial C}{\partial x} \propto \frac{C_\infty}{u_\infty}\frac{du}{dx} \tag{4}$$

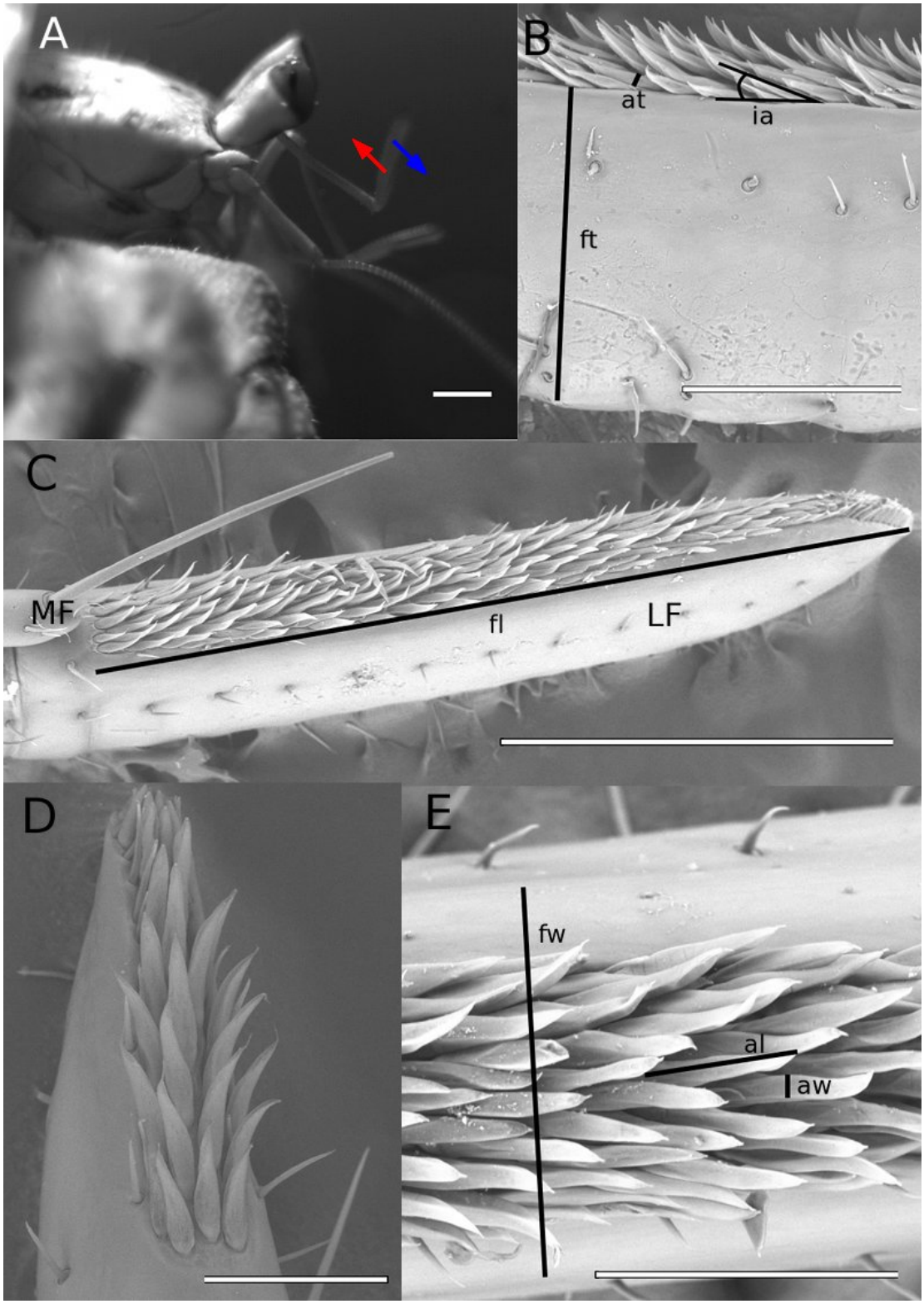

Figure 1. A: Lateral view of the anterior of *C. perlatus*, arrows indicate the direction of antennule flicking of the downstroke (blue) and return stroke (red) (scale: 1 mm). B-F: Scanning electron micrographs of antennules. B: Lateral flagellum (LF) of the antennule, lateral view, 999-mm carapace width (CW) animal, with medial flagellum (MF) (scale: 300 μm). C: 5.43-mm CW (scale: 1 mm). E: ventral view, 7.51-mm CW (scale: 500 μm). F: ventral view, 1.2-mm CW (scale: 100 μm). Morphometric measurements: fl - flagellum length, fw - flagellum width, ft - flagellum thickness, al - aesthetasc length, aw - aesthetasc width, at - antennule thickness, ia - insertion angle of aesthetasc.

If we assume the velocity gradient of a flat object in viscous flow as:

$$\frac{du}{dx} \propto \frac{u_\infty Re^{1/2}}{L} \tag{5}$$

Substituting these relationships into Fick's equation (eq. 3), we get an expression that is proportional to mass flux in laminar flow due to convection:

$$\frac{\partial C}{\partial t} \propto \frac{DC_\infty}{L} Re^{1/2} \tag{6}$$

where C_∞ is the concentration of odorant above the boundary layer. Since mass flux due to convection scales as $Re^{1/2}/L$, we can surmise that an animal with an antennule 1/10th the size of an adult antennule would capture about 70% fewer molecules.

However, if the antennules of juvenile crabs were relatively larger as compared to body size, the reduction in Re, and therefore odor capture, would be less severe. Allometric scaling has be investigated in aquatic crustaceans during sniffing (Mead et al., 1999; Mead and Koehl, 2000; Goldman and Koehl, 2001; Waldrop, 2012, 2013) and locomotion (Williams, 1994a,b). For sniffing crustaceans, allometric scaling is a key feature that allows juvenile stomatopods and crabs to retain the ability to sniff throughout growth.

As a juvenile moves from water to air, the physical properties of the fluid also change. These properties affect the movement of odor molecules in the fluid, so a change in fluid will also alter the dynamics of odor capture. Two fluid properties are of interest during this transition: the kinematic viscosity of the fluid (ν) and the molecular diffusivity of a substance in a fluid(D). Both kinematic viscosity and molecular diffusivity share the same units, and they can both be thought of as values of diffusivity; molecular diffusivity as the ability of mass to diffuse through the fluid, and kinematic viscosity as the ability of momentum to diffuse through a fluid.

The Schmidt number ($Sc = \nu/D$) describes the relative importance of momentum to mass diffusivity, and previous analyses show that the flux density of molecules is proportional to $Sc^{1/3}$ (Bird et al., 1960; Denny, 1993). The kinematic viscosity of air is approximately 15 times higher than water, and the molecular diffusivities of odorant molecules in air are typically several orders of magnitude higher than in water. Moving from water into air would illicit a large drop in Sc, so flux densities would change drastically during the juvenile's transition from water to air.

Study objectives

In this study, we characterize the changes in the antennules, aesthetascs, and flicking kinematics during ontogeny of two species of co-occurring terrestrial hermit crabs, *Coenobita rugosus* and *Coenobita perlatus*. From these measurements, we use a simple model of mass transport, which integrates both arguments of increase in body size and the transition between water and air, to infer how the odorant capture will change during growth for a variety of chemical odorants in both air and water.

METHODS AND MATERIALS

Collection and maintenance of animals

Terrestrial hermit crabs of two species, *Coenobita perlatus* H. Milne-Edwards and *Coenobita rugosus* H. Milne-Edwards, were collected on Motu Tiahura, a small island near Moorea, French Polynesia under the auspices of a government scientific permit. Individuals were maintained together in small enclosures outside for approximately 10 days and fed with breadfruit, shrimp, and coconut. After data collection was completed, they were released at the site from where they were collected in accordance with collecting permits.

Carapaces of individuals were photographed and measured for width along the widest point with ImageJ software (Abramoff et al., 2004) to the nearest 10^{-4} m as an index of body size. Each crab was marked on the dorsal surface of their shell with black permanent marker with unique identifying numbers. Animals ranged in carapace width between 0.80 and 12 mm.

Kinematics and morphometrics

Videos of antennule flicking by each crab were made for kinematic analysis. Videos were taken inside a well-ventilated room in high relative humidity ($85-90\%$) at an ambient temperature of $80-85\,^{\circ}$C.

Each animal was placed in a small enclosure (15 cm by 30 cm; 10 cm in height) that limited visual stimulation and ambient wind currents. Animals were allowed to acclimate for five to ten minutes before data collection began. A Phantom Miro high-speed camera was used to record the flicking behavior of antennules at 200 fps.

Flicking events captured on video were analyzed using Graphclick for Mac (Arizona Software, Inc.). The positions (measured to the nearest 10^{-4} m) of the distal end of each lateral flagellum were digitized. The distances traveled between each frame during each stroke were summed over the duration of the stroke, and the summation was divided by the total duration of the stroke to calculate the average speeds for the downstroke and return stroke. Three to five individual flick events were digitized and averaged per individual for each kinematic value.

One antennule from each live animal was excised and preserved on site in 70% ethanol in distilled water and transported to University of California, Berkeley for scanning electron microscopy (SEM). At UCB, antennules were fixed in 2% glutaraldehyde in 0.1 M sodium cacodylate buffer at pH 7.2 for one hour and then post-fixed in 1 percent osmium tetroxide in 0.1 M sodium cacodylate buffer at pH 7.2. Samples were dehydrated in an alcohol series and dried in a Tousimis AutoSamdri 815 Critical Point Dryer (process described by Mead et al. (1999) and Waldrop (2013). Scanning electron micrographs were taken with a Hitachi TM-1000 Environmental Scanning Electron Microscope with a 15 kV beam at various magnifications.

Morphometric measurements were taken for one antennule per crab. ImageJ (Abramoff et al., 2004) was used to measure (to the nearest 10^{-2} μm) morphological features in the scanning electron micrographs. The features of the lateral flagella and aesthetascs that were measured are diagrammed in Figure 1D and 1F. Five aesthetascs from each antennule were haphazardly chosen and measured for width, length and thickness; these measurements were averaged for each individual crab. The width, thickness, and length of the aesthetasc-bearing section of the lateral flagellum, as well as the total number of aesthetascs for each antennule, were measured only once per individual.

Statistical analysis

Natural logarithms were calculated for each morphometric and kinematic value measured and were graphed against the natural logarithm of carapace width. Regression analysis was completed with the standard statistical package in *R* to determine if a significant relationship existed between the measurement, carapace width, and species (Fox and Weisberg, 2011). The slope, intercept, species effects, and interactive effects for each measurement are reported with standard error and associate p-values (Tables 1 and 2). Significance was determined at the level $\alpha = 0.01$.

To determine whether measurements that scale with carapace width scale isometrically or allometrically, expected slopes were determined based on scaling arguments. All measurements of length were expected to have slopes equal to 1 ($\beta_0 = 1$), except the number of aesthetascs which had an expected slope of 2 as the number of aesthetascs should be proportional with an area ($\beta_0 = 2$). Slopes not equal to the expected slope for that measurement indicate allometric growth ($\beta \neq \beta_0$). To test statistical difference between slopes, the measured slope β was tested against the expected slope using a t-statistic (Waldrop, 2013). P-values were determined from a student's bimodal t-distribution with $(n-2)$ degrees of freedom at $\alpha = 0.01$.

Model of odor-capture performance

Reynolds numbers, important for determining the minimum distance required for molecules to diffuse from surrounding air, were calculated using eq. 2 and a range of values determined by the regression lines for kinematic and morphometric parameters. Antennule width was used as the characteristic length (L), stroke speed (downstroke and return stroke separately) was used as velocity relative to the object u_∞, and the value used for the kinematic viscosity of air at high humidity was $\nu = 8.55 \times 10^{-6}$ m^2 s^{-1} (Denny, 1993). Reynolds numbers were used to estimate the thickness of the boundary layer surrounding the antennule while flicking, having roughly a relationship proportional to the $Re^{-1/2}/L$. To explore the effects of scaling on boundary layer thickness, two boundary layer thicknesses were calculated: 1) the allometric relationships identified by the morphometric and kinematics analyses, and 2) an isometric relationship derived from morphometrics and kinematics of the largest animal in the study (carapace width = 0.012 m) and scaled down with a slope equal to 1 to reflect isometry.

To investigate how scaling would affect the molecular capture, we constructed a simple model based on the analysis in Denny (1993), which we reconstruct here. Combining eq. 6 with the idea that the

change in concentration is proportional to $Sc^{1/3}$ (Denny, 1993; Bird et al., 1960), the resulting equation is an expression of mass flux density due to convection (J_c):

$$J_c = \frac{0.32DC_\infty}{L} Re^{1/2} Sc^{1/3} \tag{7}$$

Since the total mass flux density to an object is due to both diffusion and convection, adding the convective and diffusive terms gives Denny's expression for total mass flux density (J):

$$J = \frac{2DC_\infty}{L} + \frac{0.64DC_\infty}{L} Re^{1/2} Sc^{1/3} \tag{8}$$

When antennule width is used as L and downstroke speed is used as u_∞, eq. 8 provides an estimate of the density flux of odorant molecules to the antennule. To measure performance of odorant capture performance, we multiplied eq. 8 by the circumference of the antennule to produce a current of odorant molecules per unit antennule length:

$$I = 4\pi DC_\infty + 1.2\pi DC_\infty Re^{1/2} Sc^{1/3} \tag{9}$$

A range of antennule widths and downstroke speeds were used to calculate I with eq. 9, based on the carapace widths of animals from which data were collected. Two versions of I were calculated: one based on allometry (I_a), and one based on isometry (I_i) following the method used to calculate isometric Re. These results are presented as the ratio I_a/I_i that is independent of initial concentration since C_∞ cancels from the eq. 9 when a ratio is calculated.

A range of diffusion coefficients was also used to explore the effects of diffusivity on I_a/I_i. This range (D = 1 x10^{-12} to 1 x10^{-5} m^2 s^{-1}) bounds a realistic range of diffusivities in air and water of odorants that have been demonstrated to illicit physiological responses in *Coenobita clypeatus* (Krang et al., 2012).

RESULTS

Scaling of morphometric measurements with carapace width

For morphological measurements, eight *C. perlatus* and 27 *C. rugosus* yielded data, ranging in carapace width from 1.2 to 12 mm. Morphometric measurements of the features of aesthetascs and lateral flagella were graphed against carapace width in Figs. 2. Table 1 is a summary of the regressions performed on these values against carapace width which includes coefficients for slope and intercept as well as multiple R^2 for each regression.

Aesthetasc widths ranged between 9.23 x10^{-6} and 2.4 x10^{-5} m, and lengths between 4.60 x10^{-5} and 1.28 x10^{-4} m. Both aesthetasc length and width scale significantly with carapace width (width: $\beta = 0.282 \pm 0.1$, dof = 31, p = 0.013; length: $\beta = 0.386 \pm 0.1$, dof = 37, p = 0.004), although the regression model seems to explain little of the variation in measurement. Aesthetasc thickness (range: 4.82 x10^{-6} to 1.69 x10^{-5} m) and the insertion angle of the aesthetascs (9.18 to 28.1 degrees) did not vary significantly with carapace width. The value of observed slope also indicate these features grow allometrically, as they are significantly different than the expected slope value of one based on isometric growth (width: $\beta_0 = 1$, $\beta = 0.282 \pm 0.1$, dof = 31, p = 2 x10^{-7}; length: $\beta_0 = 1$, $\beta = 0.386 \pm 0.1$, dof = 37, p = 3 x10^{-7}). Since both slopes are less than one, juvenile hermit crabs have relatively larger aesthetascs compared to adult animals, and aesthetascs grow more slowly during ontogeny than body size.

Several measurements of the aesthetasc-bearing section of the lateral flagellum scaled significantly with carapace width (see Table 1 for p-values). Flagellum width and thickness also scale allometrically, having slope that are significantly different than the expected slope (width: $\beta_0 = 1$, $\beta = 0.551 \pm 0.1$, dof = 21, p = 0.006; thickness: $\beta_0 = 1$, $\beta = 0.450 \pm 0.2$, dof = 32, p = 0.001). These slopes are also reflective of relatively larger antennules on small juvenile hermit crabs which grow more slowly than carapace width. However, the length of the flagellum, ranging from 7.10 x10^{-5} to 2.3 x10^{-3} m, had a slope consistent with the expected slope ($\beta_0 = 1$, $\beta = 0.905 \pm 0.2$, dof = 29, p = 0.61), indicating that the length of the antennule is isometric with body size throughout ontogeny.

The total number of aesthetascs, ranging from 23 to 267, on the lateral flagellum is proportional to the area of the array and should scale with carapace width as area scales with length; the expected slope of this relationship is two. The number of aesthetascs does scale with carapace width ($\beta = 1.32 \pm 0.2$, dof = 19, p = 6 x10^{-7}) but significantly less than the value expected from isometry ($\beta_0 = 2$, $\beta = 1.32 \pm 0.2$, dof = 19, p = 0.009). This result indicates that adult animals have relatively fewer aesthetascs in their arrays than small juveniles.

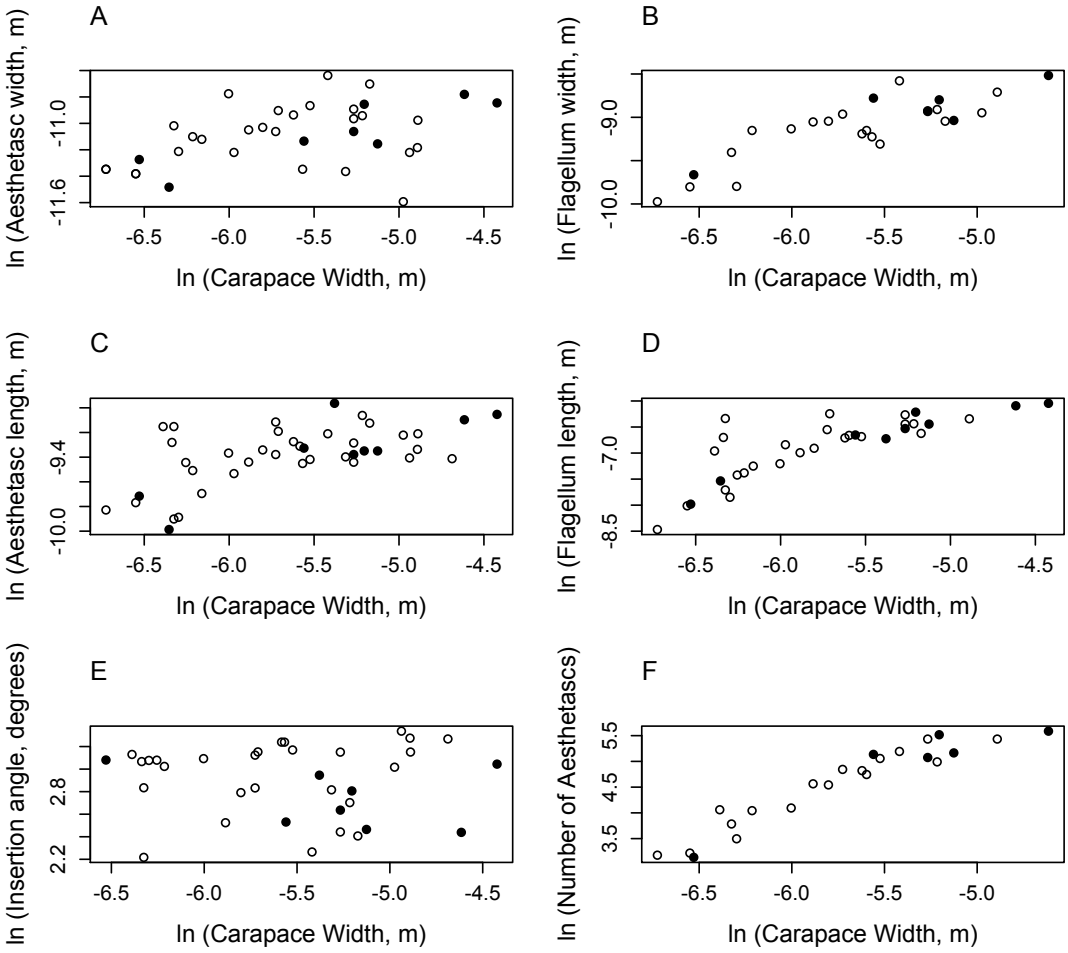

Figure 2. Natural logarithm of measurements of aesthetasc and flagellum dimensions versus natural logarithm of carapace width (m). Each measurement corresponds to the dimension illustrated in Fig. 1. Black, filled circles are measurements on *C. perlatus*; white, unfilled circles are measurements on *C. rugosus*. A: Aesthetasc width (m), B: flagellum width (m), C: aesthetasc length (m), D: flagellum length (m), E: insertion angle (degrees), and F: number of aesthetascs in array.

Scaling of kinematic measurements with carapace width

For kinematic measurements, 16 *C. perlatus* and 29 *C. rugosus* yielded data, ranging in carapace width from 0.80 to 12 mm. Kinematic measurements of antennule movement were graphed against carapace width (Fig. 3).

Downstroke speeds ranged between 7.39 $x10^{-3}$ m s^{-1} and 1.49 $x10^{-1}$ m s^{-1} and durations ranged from 5.88 $x10^{-2}$ to 1.55 $x10^{-1}$ s. Downstroke scaled significantly with carapace width ($\beta = 1.05 \pm 0.1$, dof = 41, p = 1 $x10^{-11}$). The observed slope did not differ significantly from the expected slope ($\beta_0 = 1$, $\beta = 1.05 \pm 0.1$, dof = 41, p = 0.68), indicating that downstroke speed scaled with isometry. Downstroke duration, however, was not significantly correlated with carapace width ($\beta = 0.0694 \pm 0.08$, dof = 39, p = 0.41).

Return stroke speeds ranged from 7.55 $x10^{-3}$ to 43.72 $x10^{-1}$ m s^{-1} and durations ranged between 3.67 $x10^{-2}$ to 1.53 $x10^{-1}$ s. Like the downstroke speeds, return stroke speeds increased significantly with increasing carapace width ($\beta = 1.32 \pm 0.1$, dof = 41, p = 5 $x10^{-14}$), but increase faster than predicted by isometrically ($\beta_0 = 1$, $\beta = 1.32 \pm 0.1$, dof = 41, p = 0.009). Return stroke durations were also not significantly correlated with carapace width ($\beta = 0.102 \pm 0.09$, dof = 41, p = 0.26).

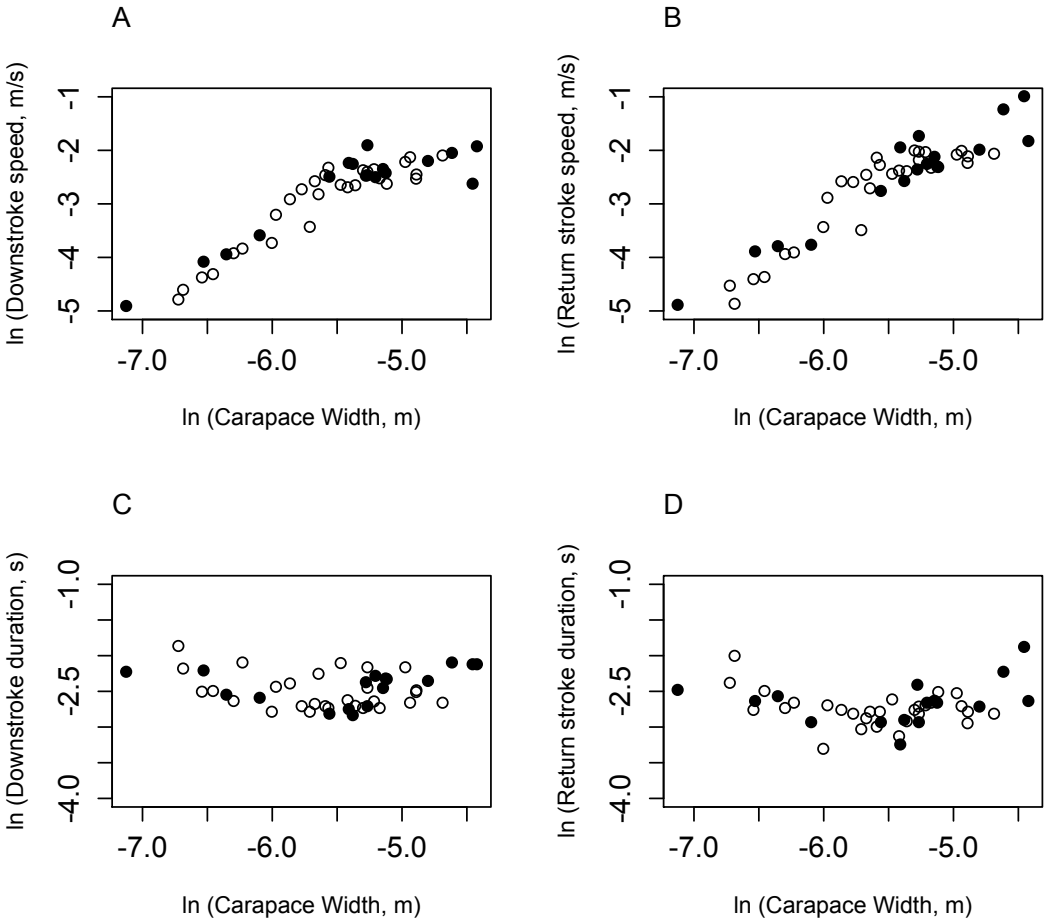

Figure 3. Natural logarithm of kinematic measurements versus natural logarithm of carapace width (m). Black, filled circles are measurements on *C. perlatus*; white, unfilled circles are measurements on *C. rugosus*. A: Downstroke speed (m s^{-1}); B: return stroke speed (m s^{-1}); C: downstroke duration (s); and D: return stroke duration (s).

Effects of scaling on molecule capture

Reynolds numbers for the downstroke (blue lines) and return stroke (red lines) are plotted against carapace width in Fig. 4A. The solid lines represent *Re* based on allometric measurements and dashed lines are *Re* calculated based on isometry. *Re* for both stroke increase during ontogeny and for allometry and isometry. For the allometric condition, downstroke *Re* range between 0.060 and 4.6 and between 0.050 and 7.9 for the return stroke. The *Re* of the isometric condition start lower for smaller animals (downstroke: 0.018, return stroke: 0.015) while ending at the same values for larger animals, resulting in a larger lifetime change.

The relative boundary layer thicknesses for the downstroke were used to create a proxy for the thickness of the attached fluid layer on the antennule during movement. Ratios were calculated by dividing the thickness based on allometry with the thickness based on isometry for each carapace width to identify relative effects of scaling; these ratios is plotted against carapace width in Fig. 4B. For the smallest animals (carapace width 0.8 mm), the ratio is 0.16, indicating that the boundary layer around an allometrically scaled antennule is 84 percent thinner than the layer around an isometrically scaled antennule. The ratios approach 1 during growth.

The ratios of odorant currents, I_a/I_i, for various diffusion coefficients are graphed against carapace width in Fig. 4C. All ratios are above 1, which indicates that antennules that scale allometrically capture more odorant molecules than antennules that scale isometrically. The magnitude of this effect depends on

the value of the diffusion coefficient, with smaller animals with allometrically scaled antennules capturing modestly more molecules (1.05 to 1.15) for higher diffusion coefficients (1 x10^{-7} to 1 x10^{-5} m^2 s^{-1}) and up to 1.8 times molecules than isometrically scaled antennules in lower diffusion coefficients (1 x10^{-12} to 1 x10^{-8} m^2 s^{-1}). The lower diffusivities are more representative of coefficients for odorant molecules in water.

Effect of species on morphometric and kinematic measurements

Species was used as a secondary predictor for the regressions of morphometric and kinematic measurements versus carapace width. Tables 1 and 2 report the coefficients and p-values associated with the effect of species, as well as the interaction between species and carapace width for each regression model. There was no significant effect of species or interactive effect between species and carapace width for any morphometric measurement examined. There were two slight effects of species in the duration of each stroke where p-values were between 0.05 and 0.01, indicating a possible difference in the duration of each stroke between species but not the speed of the antennule movement.

DISCUSSION

Effects of ontogenetic scaling on odor capture

Many crustaceans rely on flicking antennules with arrays of chemosensory aesthetascs in order to capture odor in their environments. These animals increase in size over an order of magnitude during growth, and since the fluid dynamics of odor capture rely heavily on the size and speed of the antennules during flicking, the animals' ability to capture odors may change during ontogeny. However, many aquatic crustaceans grow allometrically, which reduces the magnitude of size change (Mead et al., 1999; Waldrop, 2013) and retains function of the antennule throughout ontogeny (Mead and Koehl, 2000; Waldrop, 2012).

Although terrestrial hermit crabs do not seem to rely on the same mechanism of sniffing as aquatic crustaceans such as crabs (Waldrop, 2012), many features of their antennules and aesthetasc arrays scale allometrically in the same way. Small juveniles have relatively larger antennules and aesthetascs than adult hermit crabs, which results in much higher *Re* and thinner boundary layer than would be expected from isometry.

In this study, we used a previous analysis of mass transport to an object over flow to construct a simple model of odorant capture to infer the effects that growth would have by comparing cases of allometric growth and isometric growth. The model suggests that there could be modest improvements of odorant capture due to scaling antennule features allometrically, up to 15% higher capture rates than isometry. Since the size of an object heavily influences the thickness of the boundary layer (eqs. 1 and 2), and thus the distance diffusion must move molecules before capture, the relatively larger antennules of small juvenile crabs due to allometrically growth result in higher molecule capture compared to isometrically scaled antennules.

We also used this model to analyze the effect on the capture of different odorant molecules in both air and water through varying the diffusion coefficient D. In Fig. 4C, the cooler colors (D = 1 x10^{-7} to 1 x10^{-5} m^2 s^{-1}) represent a broad range of smaller to larger molecules diffusing in air. The effects of allometry are greater as molecules become larger because D increases. Molecules of interest are typically volatile organic compounds (dark blue to green in Fig. 4C) which have higher diffusivities than smaller molecules such as water (purple in Fig. 4C). These results suggest that allometric growth results in disproportionately greater delivery of large molecules, while providing little benefit to smaller molecules. If the reverse situation is considered, where water was being lost by diffusion away from the antennule to dry air, extra water would not be lost due to the larger antennules produced by allometry. However, this speculation should be tempered by the fact that water evaporation is complicated significantly by the effects of surface tension, which are not a part of this analysis.

Implications of allometric scaling on settlement of larvae

Olfaction is an important aspect of the transition between sea and land that terrestrial hermit crabs undergo during their lifetimes. Olfactory cues are important for predatory avoidance (Diaz et al., 1999) and possibly used to find suitable places to settle (Welch et al., 1997). There is evidence that both larvae and juvenile *Coenobita* sp. have well-developed antennules with aesthetascs and olfactory bulbs capable of processing olfactory information, indicating that competent larvae could attempt to find chemical cues in water using their antennules and aesthetasc arrays.

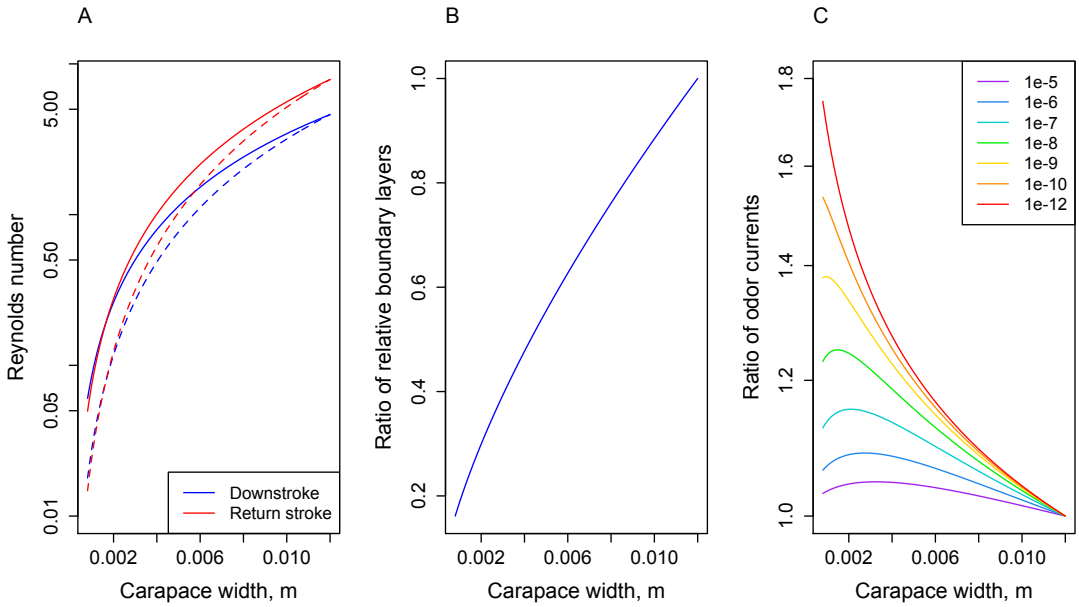

Figure 4. Calculated values based on regression lines versus carapace width. A: Reynolds numbers of antennule flicking (L = flagellum widths) on a logarithmic scale, solid lines are based on allometric relationships and dashed lines are based on isometry; B: ratio of boundary layer thicknesses predicted by allometry to isometry; and C: ratio of odor current per unit antennule length predicted by allometry to isometry using various values of D (m^2 s^{-1}).

In our model, using diffusion coefficients in Fig. 4C represented by the warmer colors (D = 1 x10^{-12} to 1x10^{-9} m^2 s^{-1}) that cover a broad range of smaller to larger molecules diffusing in water show a marked improvement for allometrically scaled antennules. Up to 75 percent more odorant molecules are captured as compared to isometrically scaled antennules for these higher values of D. Allometric scaling of olfactory antennules is likely more beneficial to settling larvae and juveniles before the water-to-air transition than juvenile crabs already living on land.

Species and habitat

Morphometric and kinematic data were collected from two species of the genus *Coenobita* which co-occur on tropical Indo-Pacific islands such as in French Polynesia. In fact, the antennules of these species are difficult to tell apart when removed from the animals except for their color (*C. perlatus* antennules are red-orange whereas *C. rugosus* are brown). No metric measured yielded a significant difference between the two species. This result could be due to phylogenetic history, it is unclear how long ago the two species diverged evolutionarily. There may also be selective pressures on performance to maintain the morphology and kinematics of the antennules.

Coenobita species often prefer different terrestrial habitats (Barnes, 1997), and we observed *C. rugosus* more often further from shore in wooded inland and *C. perlatus* more often on the near-water shore and hypothesized that this difference in habitat may lead to differences in antennule morphology and flicking kinematics since forest present a different aerodynamic environment for olfactory navigation. However, our results do not indicate such a difference, and when wind data were gathered and analyzed from both habitats where crabs were collected, no difference in wind conditions were observed (Waldrop, unpublished data).

ACKNOWLEDGEMENTS

Special thanks to M. Wright for support in the field; F. Murphy, H. Murphy, and the UC Berkeley Gump Field Station for field accommodations; M.A.R. Koehl for support and guidance; L. Miller, S. Khatri, J. Prairie, and D. Evangelista for assistance with data analysis and manuscript editing; and G. Min and the UC Berkeley Electron Microscopy Lab for assistance with microscopy.

FUNDING

This work was supported by the Virginia and Robert Gill Chair and a MacArthur Foundation Fellowship (to M. Koehl); the Reskteco and Gray Fellowships from the University of California, Berkeley Department of Integrative Biology to L. Waldrop; Sigma-Xi Grant-in-Aid of Research to the L. Waldrop; and by a Traineeship to L. Waldrop (National Science Foundation Integrative Graduate Education and Research Traineeship [DGE-0903711] to R. Full, M. Koehl, R. Dudley, and R. Fearing); and by a National Science Foundation Research and Training Grant 5-54990-2311 (to R. McLaughlin, R. Camassa, L. Miller, G. Forest, and P. Mucha).

REFERENCES

Abramoff, M., Magalhaes, P., and Ram, S. (2004). Image processing with imagej. *Biophotonics International*, 11(7):36–42.

Atema, J. (1995). Chemical signals in the marine-environment - dispersal, detection, and temporal signal analysis. *Proceedings of the National Academy of Science USA*, 92(1):62–66.

Barnes, D. (1997). Ecology of tropical hermit crabs at quirimba island, mozambique: a novel and locally important food source. *Marine Ecology Progess Series*, 161:299–302.

Beltz, B., Kordas, K., Lee, M., Long, J., Benton, J., and Sandeman, D. (2003). Ecological, evolutionary, and functional correlates of sensilla number and glomerular density in the olfactory system of decaopod crustaceans. *Journal of Comparative Neurology*, 455:260–269.

Bird, R., Stewart, W., and Lightfoot, E. (1960). *Transport Phenomena*. John Wiley and Sons, Hoboken, NJ, 1 edition.

Bliss, D. and Mantel, L. (1968). daptations of crustaceans to land - a summary and analysis of new findings. *American Zoologist*, 8(3):673.

Brodie, R. (2002). Timing of the water-to-land transition and metamorphosis in the land hermit crab coenobita compressus h. milne eddwards: evidence that settlement and metamorphosis are de-coupled. *Journal of Experimental Marine Biology and Ecology*, 272(1):1–11.

Caldwell, R. (1979). Cavity occupation and defensive behavior in the stomatopod gonodactylus- festai - evidence for chemically mediated individual recognition. *Animal Behavior*, 27:194–201.

Denny, M. (1993). *Air and Water: The Biology of Life's Media*. Princeton University Press, Princeton, NJ.

Diaz, H., Orihuela, B., Forward, R., and Rittschof, D. (1999). Orientation of blue crab, callinectes sapidus (rathbun), megalopae: Responses to visual and chemical cues. *Journal of Experimental Marine Biology and Ecology*, 233(1):25–40.

Dusenbery, D. (1992). *Sensory ecology: How organisms acquire and respond to information.* W.H. Freeman.

Ferner, M., Smee, D., and Chang, Y. (2005). Cannibalistic crabs respond to the scent of injured conspecifics: Danger or dinner? *Marine Ecology Progess Series*, 300:193–200.

Fox, J. and Weisberg, S. (2011). *An R Companion to Applied Regression*. Sage, Thousand Oaks, CA, USA, 2nd edition.

Gherardi, F. and Tricarico, E. (2007). Can hermit crabs recognize social partners by odors? and why? *Marine and Freshwater Behavioral Physiology*, 40(3):201–212.

Gherardi, F., Tricarico, E., and Atema, J. (2005). Unraveling the nature of individual recognition by odor in hermit crabs. *Journal of Chemical Ecology*, 31(12):2877–2796.

Ghiradella, F., Case, J., and Cronshaw, J. (1968). Structure of aesthetascs in selected marine and terrestrial decapods - chemoreceptor morphology and environment. *American Zoologist*, 8(3):603–621.

Gleeson, R. (1980). Pheromone communication in the reproductive-behavior of the blue-crab, callinectes-sapidus. *Marine Behavior and Physiology*, 7(2):119–134.

Gleeson, R. (1982). Morphological and behavioral identification of the sensory structures mediat- ing pheromone reception in the blue-crab, callinectes-sapidus. *Biological Bulletin*, 163(1):162–171.

Goldman, J. and Koehl, M. (2001). Fluid dynamic design of lobster olfactory organs: High speed kinematic analysis of antennule flicking by panulirus argus. *Chemical Senses*, 26(4):385–398.

Goldman, J. and Patek, S. (2002). Two sniffing strategies in palinurid lobsters. *Journal of Experimental Biology*, 205(24):3891–3902.

Greenaway, P. (2003). Terrestrial adaptations in the anomura (crustacea: Decapoda). *Memoirs of Museum Victoria*, 60(1):13–26.

Harzsch, S. and Hansson, B. (2008). Architecture of the central olfactory pathway in a terrestrial hermit crab with a superb aerial sense of smell, coenobita clypeatus (crustacea, anomura, coeno- bitidae). *Journal of Morphology*, 269(12):1463.

Hazlett, B. (1969). Individual recognition and agonistic behaviour in pagurus bernhardus. *Nature*, 222(5190):268–269.

Keller, T., Powell, I., and Weissburg, M. (2003). Role of olfactory appendages in chemically medi- ated orientation of blue crabs. *Marine Ecology Progess Series*, 261:217–31.

Koehl, M. (2006). The fluid mechanics of arthropod sniffing in turbulent odor plumes. *Chemical Senses*, 31(2):93–105.

Krang, A., Knaden, M., Steck, K., and Hansson, B. (2012). Transition from sea to land: olfactory function and constraints in the terrestrial hermit crab coenobita clypeatus. *Proceedings of the Royal Society B*, 279:3510–3519.

Lecchini, D., Mills, S., Brie, C., Maurin, R., and Banaigs, B. (2010). Ecological determinants and sensory mechanisms in habitat selection of crustacean postlarvae. *Behavioral Ecology*, 21(3):599–607.

Mead, K. and Koehl, M. (2000). Stomatopod antennule design: The asymmetry, sampling effi- ciency and ontogeny of olfactory flicking. *Journal of Experimental Biology*, 203(24):3795–3808.

Mead, K., Koehl, M., and O'Donnell, M. (1999). Stomatopod sniffing: The scaling of chemosen- sory sensillae and flicking behavior with body size. *Journal of Experimental Marine Biology and Ecology*, 241(2):235–261.

Moore, P., Atema, J., and Gerhardt, G. (1991). Fluid-dynamics and microscale chemical movement in the chemosensory appendages of the lobster, homarus-americanus. *Chemical Senses*, 16(6):663–674.

Moore, P. and Crimaldi, J. (2004). Odor landscapes and animal behavior: tracking odor plumes in different physical worlds. *Journal of Marine Systems*, 49:55–64.

Pardieck, R., Orth, R., Diaz, R., and Lipcius, R. (1999). Ontogenetic changes in habitat use by postlarvae and young juveniles of the blue crab. *Marine Ecology Progess Series*, 186:277–238.

Schmidt, B. and Ache, B. (1979). Olfaction: responses of a decapod crustacean are enhanced by flicking. *Science*, 205:204–206.

Schuech, R., Stacey, M., Barad, M., and Koehl, M. (2012). Numerical simulations of odorant detection by biologically inspired sensor arrays. *Bioinspiration and Biomimetics*, 7(1):016001.

Shabani, S., Kamio, M., and Derby, C. (2009). Spiny lobsters use urine-borne olfactory signaling and physical aggressive behaviors to influence social status of conspecifics. *Journal of Experimental Biology*, 212(15):2464–2474.

Skog, M. (2009). Male but not female olfaction is crucial for intermolt mating in european lobsters (homarus gammarus l.). *Chemical Senses*, 34(2):159–169.

Stacey, M., Mead, K., and Koehl, M. (2002). Molecule capture by olfactory antennules: Man- tis shrimp. *Journal of Mathematical Biology*, 44(1):1–30.

Stensmyr, M., Erland, S., Hallberg, E., Wallen, R., Greenaway, P., and Hansson, B. (2005). Insect- like olfactory adaptations in the terrestrial giant robber crab. *Current Biology*, 15(2):116–121.

Thacker, R. (1996). Food choices of land hermit crabs (coenobita compressus h. milne edwards) depend on past experience. *Journal of Experimental Marine Biology and Ecology*, 199:179–191.

Vogel, S. (1994). *Life in Moving Fluids: The Physical Biology of Flow*. Princeton University Press, Princeton, NJ.

Waldrop, L. (2012). *The fluid dynamics of odor capture by crabs*. PhD thesis, University of California, Berkeley.

Waldrop, L. (2013). Ontogenetic scaling of the olfactory antennae and flicking behavior of the shore crab, hemigrapsus oregonensis. *Chemical Senses*, 38(6):541–550.

Welch, J., Rittschof, D., Bullock, T., and Forward, R. (1997). Effects of chemical cues on settlement behavior of blue crab callinectes sapidus postlarvae. *Marine Ecology Progess Series*, 154:143–153.

Williams, T. (1994a). Locomotion in developing artemia larvae: Mechanical analysis of antennal propulsors based on large-scale physical models. *Biological Bulletin*, 187(2):156–163.

Williams, T. (1994b). A model of rowing propulsion and the ontogeny of locomotion in artemia larvae. *Biological Bulletin*, 187(2):164–173.

Zimmer, R. and Butman, C. (2000). Chemical signaling processes in the marine environment. *Biological Bulletin*, 198(2):168–187.

Measurement	Slope, β		Intercept		Species		Interaction		Multiple	Isometry	
	Coef±SE	p-value	Coef±SE	p-value	Coef±SE	p-value	Coef±SE	p-value	R2	β_0	p-value
Aesthetasc ...											
width	0.282±0.1	0.013 *	-9.56±0.6	$2x10^{-16}$ **	-0.870±0.7	0.23	-0.165±0.1	0.21	0.24	1	$2x10^{-7}$ **
length	0.386±0.1	0.004 **	-7.28±0.5	$5x10^{-16}$ **	-0.954±0.7	0.15	-0.1831±0.1	0.13	0.41	1	$3x10^{-7}$ **
thickness	0.267±0.2	0.19	-9.87±1	$2x10^{-10}$ **	-1.85±1	0.16	-0.300±0.2	0.22	0.15	1	$1x10^{-3}$ **
insertion angle	-0.128±0.2	0.50	2.07±1	0.045 *	1.37±1	0.26	0.2163±0.2	0.33	0.10	0	0.49
Lateral flagellum											
width	0.551±0.2	0.001 **	-5.99±0.8	$2x10^{-7}$ **	0.0409±1	0.97	0.0131±0.2	0.94	0.73	1	0.005 **
length	0.905±0.2	$3x10^{-5}$ **	-1.82±1	0.077	0.233±1	0.86	0.00804±0.2	0.97	0.69	1	0.61
thickness	0.450±0.2	0.006 **	-5.60±0.8	$1x10^{-7}$ **	-0.964±1	0.37	-0.197±0.2	0.32	0.28	1	0.001 **
number of aes.	1.32±0.2	$6x10^{-7}$ **	12.1±1	$2x10^{-10}$ **	0.311±1	0.80	0.0322±0.2	0.89	0.91	2	0.001 **

Table 1. Summary of regressions performed on morphometric measurements. Regression model used was natural log (measurement) vs. natural log (carapace width in meters)*Species. Widths, lengths, and thicknesses are in meters; angle of aesthetasc with antennule in degrees. Slopes, intercepts, species (*C. rugosus*), and interaction between carapace width and species (*C. rugosus*) are reported as coefficients with their standard errors and p-values. Isometry column gives the expected slope of the regression line if the measurement grow isometrically with carapace width, and the isometry p-value which tests the hypothesis that values grow isometrically ($\beta = \beta_0$). * indicate significance at level p less than 0.05, ** indicates significance at level p less than 0.01.

Measurement	Slope, β		Intercept		Species		Interaction		Multiple	Isometry	
	Coef±SE	p-value	Coef±SE	p-value	Coef±SE	p-value	Coef±SE	p-value	R2	β_0	p-value
Downstroke ...											
speed	1.05±0.1	$1x10^{-11}$ **	2.93±0.6	$2x10^{-5}$ **	1.37±0.9	0.132	0.249±0.2	0.13	0.84	1	0.68
duration	0.0694±0.08	0.41	-2.05±0.5	$6x10^{-5}$ **	-1.17±0.7	0.082	-0.199±0.1	0.01*	0.09	–	–
Return stroke											
speed	1.32±0.1	$5x10^{-14}$ **	4.66±0.7	$9x10^{-9}$ **	0.625±0.9	0.50	0.116±0.17	0.49	0.87	1	0.009**
duration	0.102±0.09	0.26	-2.10±0.5	$1x10^{-4}$ **	-1.41±0.7	0.05	-0.238±0.1	0.066	0.11	–	–

Table 2. Summary of regressions performed on kinematic measurements. Regression model used was natural log (measurement) vs. natural log (carapace width in meters)*Species. Speeds are measured in meters per second, durations are in seconds. Slopes, intercepts, species (*C. rugosus*), and interaction between carapace width and species (*C. rugosus*) are reported as coefficients with their standard errors and p-values. Isometry column gives the expected slope of the regression line if the measurement grow isometrically with carapace width, and the isometry p-value which tests the hypothesis that values grow isometrically ($\beta = \beta_0$). * indicate significance at level p less than 0.05, ** indicates significance at level p less than 0.01.